Rigid polyurethane foam composites with vegetable filler for application in the cosmetics industry

Milena Zieleniewska[1), *)], Leonard Szczepkowski[2)], Małgorzata Krzyżowska[3)], Michał K. Leszczyński[4)], Joanna Ryszkowska[1)]

DOI: dx.doi.org/10.14314/polimery.2016.807

Abstract: This study was designed towards the development of rigid polyurethane foam (RPURF) composites for application in the cosmetics industry using ground hazelnut shell waste as filler. Additionally, the influence of the filler content on the structure of the composites, as well as on their physico-mechanical, thermal, and biological properties was investigated. The particle size distribution and chemical structure of the natural filler, was examined. The synthesized foams were analyzed using a variety of techniques such as infrared spectroscopy (FT-IR), thermogravimetric analysis (TGA), differential scanning calorimetry (DSC), and scanning electron microscopy (SEM). Furthermore, the apparent density, water absorption, dimensional stability, compressive strength, and resistance to aging of the materials were determined. Due to the proposed application, the toxicity analysis of the synthesized materials was essential. The conducted research resulted in the development of the composition and preparation procedure for the synthesis of rigid polyurethane foam biocomposites incorporating a high content of ground hazelnut shell as filler.

Keywords: rigid polyurethane foams, renewable sources, hazelnut shells, biocomposites.

Kompozyty sztywnych pianek poliuretanowych z napełniaczem pochodzenia roślinnego do zastosowań w przemyśle kosmetycznym

Streszczenie: Otrzymano kompozyty sztywnych pianek poliuretanowych (RPURF) z udziałem odpadowych łupin orzecha laskowego, odpowiednie do zastosowań w przemyśle kosmetycznym. Określono wpływ zawartości napełniacza na strukturę, właściwości fizykomechaniczne, termiczne oraz biologiczne wytworzonych materiałów. Przeanalizowano wymiary cząstek oraz budowę chemiczną napełniacza. Pianki RPURF scharakteryzowano za pomocą spektroskopii w podczerwieni (FT-IR), analizy termograwimetrycznej (TGA), różnicowej kalorymetrii skaningowej (DSC), skaningowej mikroskopii elektronowej (SEM). Ponadto określono gęstość pozorną kompozytów, ich chłonność wody, stabilność wymiarową, wytrzymałość na ściskanie oraz odporność na warunki starzeniowe. Ze względu na przewidywaną aplikację oceniono też toksyczność pianek. Na podstawie wyników badań opracowano skład oraz metodę wytwarzania biokompozytów sztywnych pianek poliuretanowych z dużym udziałem napełniacza pochodzenia naturalnego w postaci zmielonych łupin orzecha laskowego.

Słowa kluczowe: sztywne pianki poliuretanowe, źródła odnawialne, łupina orzecha laskowego, biokompozyty.

Rigid polyurethane foams (RPURFs) are commonly used as lightweight, thermal insulating, construction materials. In 2013, *ca.* 26 % of the 16 million tons of global polyurethane production was related to RPURF materials [1] and this fraction is estimated to increase by a further 5.3 % by 2020. Apart from thermal insulation materials, the applications of RPURFs also include the cosmetics industry, which employs RPURFs for the production of pumices [2], using mostly materials with a closed cell structure formed by crosslinked macromolecules and exhibiting densities in the range of 30–90 kg/m^3. Compared to other insulating materials such as polystyrene foam or mineral wool, the RPURFs are relatively expensive materials. Therefore, a substantial effort has been devoted to reduce the costs, for example by the synthesis of RPURFs using renewable resources [3–5], which can be applied for the production of polyols [6] or used as natural fillers [7, 8].

[1)] Warsaw University of Technology, Faculty of Materials Science and Engineering, Wołoska 141, 02-507 Warsaw, Poland.
[2)] FAMPUR Adam Przekurat company, Gersona 40/30, 85-305 Bydgoszcz, Poland.
[3)] Military Institute of Hygiene and Epidemiology, Kozielska 4, 01-163 Warsaw, Poland.
[4)] Polish Academy of Sciences, Institute of Physical Chemistry, Kasprzaka 44/52, 01-224 Warsaw, Poland.
[*)] Author for correspondence; e-mail: milenazieleniewska@wp.pl

The solutions developed within the research concerning bio-based RPURFs are often implemented by industry. Natural fillers such as flax, sisal, and jute have been applied in the production of RPURFs for the automotive industry for many years [9]. Wood is another example of a natural filler applied in RPURF production [10].

One of the most interesting and profitable sources of natural fillers is biodegradable waste generated by the agricultural and food industries, such as the inedible parts of plants and vegetables. It would be especially beneficial to use waste-based natural fillers as an alternative to the currently used ones since the resources spent on the cultivation of flax, sisal, and jute could be reattributed to the food industry. One of the most promising types of food and agriculture waste materials for RPURF fillers are the lignified parts of plants such as various shells and husks [11], which consist of cellulose, hemicellulose, lignin, proteins, waxes, resins, and pigments [12]. The shells of various nuts such as walnuts, hazelnuts, and pistachios could be potential candidates for natural fillers considering the fact that powdered walnut shells have been commercially available from JRS Rettenmaier & Söhne GmbH + Co KG for several years. The total annual production of walnuts in Poland was 4.2 thousands of tonnes in 2012 [13]. The cultivation of hazelnuts in Poland is mainly located in the Lubelskie Region and occupies an area of more than 3000 ha [14]. The hazelnuts are utilized in a variety of industries including food, confectionery, baking, pharmaceutical and cosmetics industry [15], which generates a significant demand, as well as a substantial amount of shells as a waste stream.

Ground hazelnut shells have been applied as fillers in composite materials for many years [16, 17]. Balart *et al.* [18] analyzed the mechanical and thermal properties of poly(lactic acid) (PLA) and ground hazelnut shell composites with plasticizers based on epoxidized linseed oil (ELO). According to the authors, the addition of ELO resulted in a plasticization effect as evidenced by improved ductile properties and easier manufacturing while the mechanical properties were enhanced due to the coupling between the filler and PLA. Moreover, Salasinska *et al.* [11] presented a comprehensive analysis of the physical, mechanical, and thermal properties of waste polyethylene composites with natural fibers and hazelnut shell fillers, which indicated the possibility of introducing valuable construction properties by the proper physical modification of waste polyethylene. Another contribution to the field by Matejka *et al.* [19] concerns the combination of jute fibers and powdered hazelnut shells as natural fillers for organic friction composites. The paper presents the possibility of a significant improvement of friction-wear performance by the application of natural fillers, which could induce further developments in the field of eco-friendly friction composites.

The requirements for cosmetic pumices fabricated using RPURFs are similar to natural pumices made of igneous rocks or quartz. Polyurethane pumices exhibit favorable properties for this type of application and additional qualities can be introduced by the utilization of ground hazelnut shells as filler material.

The aim of this study was to verify the possibility of synthesizing RPURFs physically modified by the introduction of ground hazelnut shells (HZS) as a natural filler with particular interest in the application of the resulting composites as cosmetic pumices with peeling qualities.

EXPERIMENTAL PART

Materials

In the synthesis of RPURF composites, the following substrates have been used:

– Rokopol G500 [poly(oxypropylene triol) based on glycerin with a hydroxyl value of 300 mg KOH/g, number average molar mass of 560 g/mol and a water content of 0.10 wt % as supplied by PCC Rokita, Poland];

– Polios 420 PET (aromatic polyester with a hydroxyl value 420 mg KOH/g, number average molar mass of 400 g/mol as supplied by Purinova, Poland);

– TEGOSTAB® B 4900 (silicone surfactant produced by Evonik Industries, Germany);

– amine-type catalyst, water was used as a blowing agent;

– Ongronat® TR 4040 [mixture of methylene diphenyl diisocyanate (MDI) isomers and oligomeric MDI, containing 32.6 wt % of free isocyanate groups as supplied by BorsodChem company];

– Hazelnut shells (HZS, a waste product from the food and agriculture industry) was supplied by an industrial partner involved in the processing of nuts. The natural filler was mechanically ground using the MUKF-10 mill (Młynpol company). In order to remove the adsorbed water, the filler was subsequently dried at 70 °C until no further loss of mass was observed.

Synthesis of the composites of rigid polyurethane foams

A one-step method was used in the synthesis of the porous polyurethane materials. Polyols and the modifiers (polyol premix) were mixed using a mechanical stirrer at 1000 rpm for 60 s. Then, the HZS filler was introduced to the polyol premix in the quantities presented in Table 1 and stirred at 200 rpm for 30 s. Subsequently, the isocyanate was added and the mixture was stirred at 1000 rpm for 8 s. The mixtures were poured to open molds where free rise foaming occurred in a vertical direction. The resulting foams were annealed for 30 min at 70 °C. The materials were then conditioned at 22 °C and 50 % relative humidity for 24 h. The resulting foams were removed from the molds and cut into smaller samples after two weeks. In order to obtain non-collapsing and stable foams, the isocyanate index was adjusted to the level of 106. The synthesis of the RPURFs was performed in the laboratory of the FAMPUR Adam Przekurat company.

T a b l e 1. The natural filler content in the analyzed materials

Sample	Amount of the natural filler in the polyol premix wt %
0 HZS	0
4 HZS	4
12 HZS	12
19 HZS	19
25 HZS	25

Methods of testing

– Ground HZS filler was subjected to sieve analysis in order to determine the grain size distribution according to the Polish standard PN-EN 933-10:2002. Sieves with meshes of: 0.032, 0.045, 0.063, 0.125, 0.15, 0.18, 0.3, 0.42, 0.85 and 2 mm were used in the process.

– The chemical composition of the filler material was investigated: the raw fat content was determined by Soxhlet extraction in chloroform ($CHCl_3$), the lignin content was analyzed according to the PN-92/P-50092 standard, the cellulose content was determined using the Seifert method according to the PN-92/P-50092 standard which was also applied in the determination of the hemicellulose content as a difference between the amounts of holocellulose and cellulose. The analyses of the HZS filler were performed at the Department of Wood Science and Wood Preservation, Warsaw University of Life Sciences.

– The chemical constitution of the RPURFs was determined based on the infrared absorption spectra recorded using a Nicolet 6700 spectrophotometer (Thermo Electron Corporation) equipped with an ATR (attenuated total reflection) unit. Each sample was scanned 64 times in the wave number range of 4000–400 cm^{-1}. The hydrogen bonding index (*R*) and the degree of phase separation (*DPS*) of the examined RPURFs were calculated based on the FT-IR spectroscopy results in order to describe the content of rigid segments hydrogen-bonded to other parts of the polymer matrix [2, 20, 21]. The results were analyzed using Omnic Spectra 2.0 software (Thermo Nicolet).

– The structure of synthesized foams was also investigated using indirect methods: differential scanning calorimetry (DSC) and thermogravimetric analysis (TGA). DSC measurements were performed using the differential scanning calorimeter DSC Q1000 (TA Instruments) under a helium atmosphere and using hermetic aluminum pans. Samples (5 ± 0.2 mg) were heated at the 10 °C/min rate then cooled at the 5 °C/min rate and finally heated at the 10 °C/min rate in the temperature range -90 °C to 220 °C. TGA analysis was performed with the Q500 analyzer (TA Instruments) using 10 ± 1 mg of samples which were heated from 25 °C to 1000 °C at the rate of 10 °C/min. The results were processed using the Universal Analysis 2000 software (4.7A version, TA Instruments).

– The porous structure of the composites was analyzed using scanning electron microscopy (SEM Hitachi TM3000). The 5 x 5 x 3 mm samples were dusted with gold using the Polaron SC7640 sputter coater in order to introduce the necessary electron conductivity for SEM imaging. The dusting was performed for 100 s at 6 mA current intensity.

– The apparent density tests were performed in accordance to the PN-EN ISO 845:2010 standard. The water absorption and dimensional stability in water at 40 °C were also determined in order to analyze the properties of the obtained materials in conditions characteristic to the application of cosmetic pumices. Water absorption was determined using the PN-C-89084:1993 standard.

– The aging test of the foam materials was carried out at an elevated temperature using an aging chamber. The test was conducted at 120 °C for 48 h.

– The compressive strength was determined according to the PN-93/C-89071 (ISO 844) standard. Samples were subjected to a compressive deformation of 10 %. The 50 x 50 x 25 mm samples were tested in the orientation parallel to the foam growth direction.

– The human monocyte and keratinocyte cell lines THP-1, as well as JC-1 dye (5,5',6,6'-tetrachloro-1,1',3,3'-tetraethyl-imidacarbocyanine iodide) were used in order to verify the toxicity of the obtained composites. The cells were initially incubated with samples for 24 h followed by measurements of the decrease of the mitochondrial potential by application of a flow cytometry technique using FACS Calibur (Beckton Dickinson, Franklin Lakes, NJ, USA). Based on the reference material sample (polystyrene surface), a statistically relevant amount of cells with decreased mitochondrial potential, excluding the samples from further applications, was determined at the level of 20 %. The toxicity assessments were performed at the Military Institute of Hygiene and Epidemiology, Poland.

– The viability of the cells was analyzed using the neutral red test. The cells were cultivated in contact with the examined materials for 24 h, collected by centrifugation, washed with phosphate buffered saline (PBS), centrifuged again and transferred to freshly prepared substrate (RPMI 1640, serum, antibiotics) with addition of 10 % of neutral red dye. Cells were incubated for 2 h and then fixed using 0.1 % $CaCl_2$ and 0.5 % formaldehyde. The dye was released using 1 % acetic acid in 50 % ethanol. Absorbance was measured using the Fluostar Omega (BMG Labtech, Germany) counter at 540 nm. The results were calculated as a percentage of living cells compared to the reference material (100 %).

RESULTS AND DISCUSSION

Analysis of the HZS filler

The grain size analysis results, which are presented in Fig. 1, indicates fine fragmentation of the filler as 90.1 % of the sample exhibits a grain size below 63 μm.

The analysis of the chemical composition of the HZS filler allowed for the determination of the contents of cel-

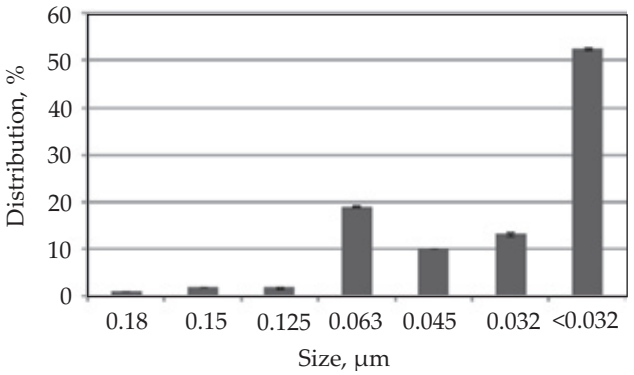

Fig. 1. Grain size analysis of the HZS

lulose (37.8 ± 0.26 %), hemicellulose (20.3 ± 0.34 %), lignin (38.7 ± 0.24 %), and raw fat (1.9 ± 0.37 %).

The chemical constitution analysis of the materials

The analysis by Fourier Transform Infrared Spectroscopy (FT-IR) confirmed the presence of chemical groups characteristic for rigid polyurethane foams. The spectra of all synthesized composites are presented in Fig. 2.

The presented spectra indicate the presence of the symmetric and asymmetric stretching vibrations of the N-H groups from the urethane moieties, which are visible in the wave number range 3305–3297 cm^{-1}, while the signals at 1512–1511 cm^{-1} represent the scissoring vibrations of these groups. Bands observed at 2926–2917 cm^{-1} and 2873–2869 cm^{-1} are related to the symmetric and asymmetric stretching vibrations of the C-H groups in the methylene moieties and the scissoring vibrations of the C-H groups are observed through signals at 1456––1450 cm^{-1}. The unreacted N=C=O groups are also visible in the low intensity signal at 2277–2271 cm^{-1}, which is commonly observed in the case of materials synthesized with an excess of the isocyanate compared to the polyol. The carbonyl C=O groups in the urethane moieties are represented by bands in the 1717–1712 cm^{-1} range [22], while the signal at 1595 cm^{-1} indicates the presence of aromatic rings originating from the isocyanate. The isocyanate trimerisation products (PIR – polyisocyanurate) are present in the samples as demonstrated by the band at 1411 cm^{-1} [23]. The signals in the 1219–1216 cm^{-1} range are related to the stretching vibrations of the C-N groups present in the polyurethanes. The multiplet bands in the range of 1250–1000 cm^{-1} are correlated with the vibrations of the flexible segments of the samples. The results of FT-IR analysis are presented in Table 2. The observed differences in band shifts are related to changes in the chemical structure of the foam materials resulting from the introduction of various amounts of the natural filler.

The resulting values of hydrogen bonding index (*R*) and degree of phase separation (*DPS*) are presented in Table 3.

Introduction of the ground hazelnut shell favors the formation of hydrogen bonds connecting the rigid segments of the foams as indicated by the increase of the *R* index. The rearrangement of the rigid segments in relation to the flexible segments caused by the presence of the HZS filler resulted in an increased degree of phase separation and enhanced physical crosslinking in the examined materials. The material with 4 wt % filler content in the polyol premix (4 HZS) was characterized with the highest degree of phase separation compared to the reference sample (0 HZS). Further increasing of the amount of filler resulted in the gradual decrease of the degree of phase separation in the polymer matrix.

Thermal analysis of the foams

Analysis of the macromolecular structure of the synthesized materials was conducted using indirect methods such as DSC and TGA. The DSC analysis was performed in a heating – cooling – heating cycle. The obtained results are presented in Fig. 3.

The DSC curves of the first heating cycle exhibited the presence of an endothermal transition peak related to the

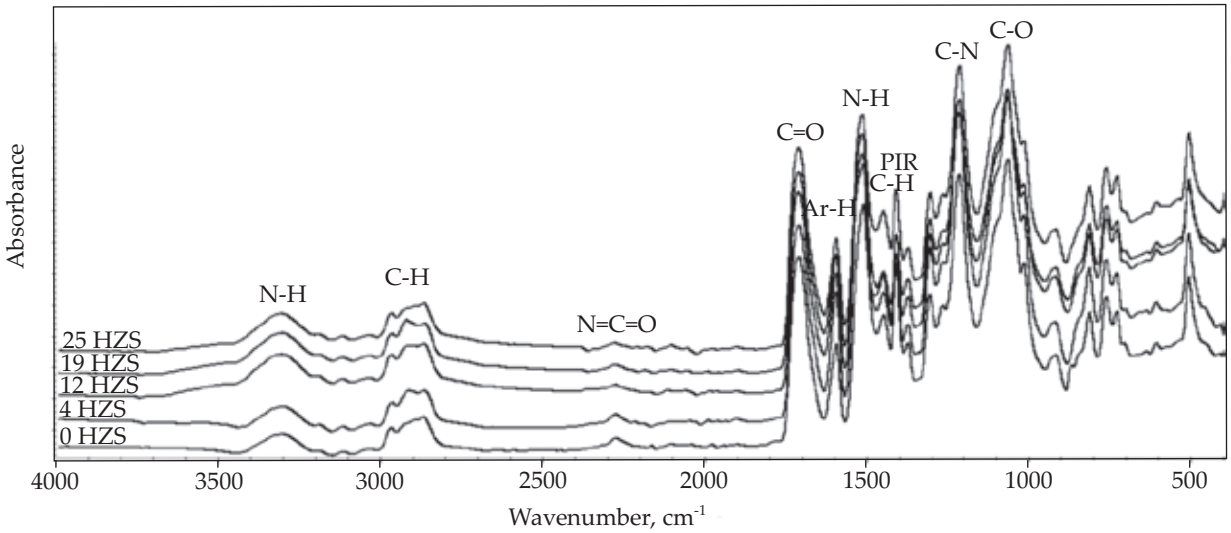

Fig. 2. FT-IR spectra of the analyzed materials

T a b l e 2. Comparison of the bands observed in FT-IR spectra of the examined materials

0 HZS	4 HZS	12 HZS	19 HZS	25 HZS	bond (vibration)
Wavenumber, cm^{-1}					
3305	3297	3299	3299	3305	N-H (stretching)
2917	2920	2926	2923	2925	C-H (asymmetric stretching)
2870	2873	2869	2875	2871	C-H (symmetric stretching)
2272	2275	2271	2273	2272	N=C=O (stretching)
1716	1717	1713	1716	1712	C=O (stretching)
1595	1595	1595	1595	1595	Ar-H (deformation)
1511	1508	1512	1511	1511	N-H (scissoring)
1453	1456	1454	1453	1450	C-H (scissoring)
1411	1411	1411	1411	1411	PIR (deformation)
1218	1216	1219	1218	1219	C-N (stretching)
1065	1066	1067	1067	1067	C-O (stretching)

T a b l e 3. Results of the degree of phase separation and hydrogen bond index analysis

Sample	*R*	*DPS*, %
0 HZS	0.986	49.6
4 HZS	1.238	55.3
12 HZS	1.194	54.4
19 HZS	1.158	53.7
25 HZS	1.063	51.5

T a b l e 4. Results of the DSC analysis of the examined materials

Sample	T_g, °C	ΔH_d, J/g
0 HZS	87	31.5
4 HZS	86	31.6
12 HZS	87	45.1
19 HZS	78	54.1
25 HZS	82	54.6

rearrangement of the hard phase, which was attributed to the dissociation of the hydrogen bonds in the hard phase. The change in enthalpy ΔH_d related to this transition was calculated based on the DSC curve. The glass transition of the hard phase (T_g) was observed in the thermograms of the second cycle of heating as an inflexion of the curve. The glass transition temperature of the foams was observed in the range of 78–87 °C. The results of the DSC thermogram analysis are presented in Table 4.

The foam properties were also investigated by analysis of the thermal degradation process (Fig. 4), which exhibited a multi-step characteristic. The DTG (derivative of the sample mass) curve included three peaks, indicating various transformation rates of processes occurring in each of the steps. Based on the TGA curves, the following parameters were determined:

– temperature of the 2 % mass loss ($T_{2\,\%}$) and 5 % mass loss ($T_{5\,\%}$),

– temperature of the maximum degradation rate for the three decomposition steps (T_1–T_3),

– mass of the residue after heating at 950 °C (R_{950}).

The results of the TG and DTG curve analysis are presented in Table 5.

Introduction of the natural filler results in a decrease of the 2 % mass loss temperature, which is related to the evaporation of the easily volatilized substances present in the filler. The temperature of the 5 % mass loss, commonly considered as the thermal degradation onset, is

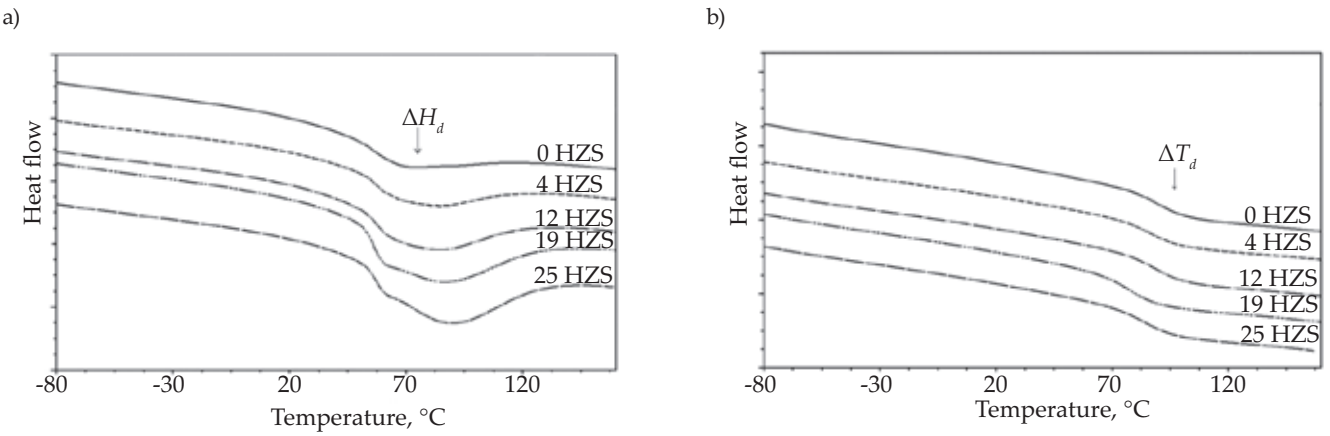

Fig. 3. DSC thermograms: a) the first, b) the second cycle of heating; the curves were moved apart along the *y* axis for clarity

T a b l e 5. Results of the TG and DTG analysis of the foams

Sample	$T_{2\ \%}$, °C	$T_{5\ \%}$, °C	T_1, °C	T_2, °C	T_3, °C	R_{950}, %
0 HZS	213	244	309	402	454	11.9
4 HZS	211	245	306	401	456	12.2
12 HZS	198	244	305	400	453	12.7
19 HZS	195	247	311	397	456	13.9
25 HZS	184	245	309	392	464	15.2

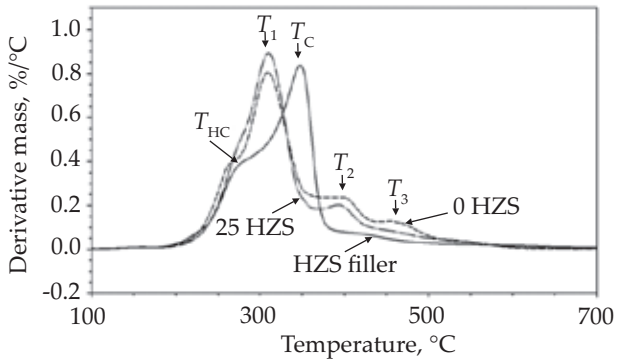

Fig. 4. Example DTG curves of the foams

contained in the 244–247 °C range for all examined materials. In all materials, the first decomposition step was observed in the temperature range 200–385 °C with the maximum thermal degradation rate (T_1) temperatures in the range 305–311 °C. This result indicates the overlapping of the signals related to the degradation of the urethane and urea bonds in the rigid segments [24, 25] and the signals connected to the degradation of the soft phase containing the Rokopol G500 polyol (the maximum degradation temperature of the polyol is 318 °C). Hemicellulose and cellulose present in the natural filler also decompose in the same temperature range (T_{HC} and T_C, respectively – Fig. 4). The maximum of the thermal degradation rate of the filler is 347 °C and can be related to the decomposition of the α-cellulose [26, 27, 28]. The decomposition of the hemicellulose appears as a shoulder of the main peak at 280 °C. Thermal degradation of the lignin present in the HZS filler occurs in a broad temperature range of 200 °C to 500 °C, which overlaps with the decomposition signals originating from other ingredients of the material [29].

The second step of the composite thermal decomposition (T_2) occurs at 392–402 °C and can be related to the degradation of the soft phase containing Polios 420 PET polyol (maximum thermal degradation rates at 370 °C and 420 °C). The third foam degradation step involves further decomposition of the organic residue originating from rigid and flexible segments, as well as from the filler.

Structural analysis of the polyurethane foams

The synthesized materials exhibited various pore structures, depending on the natural filler content used in the synthesis, as evidenced by SEM imaging. The average pore size and pore size distribution were larger in the case of greater filler loading (25 HZS). The observations are probably related to the increasing viscosity of the polyol premix with the addition of HZS filler. The obtained results indicate the ability to adjust the pore size of the composites by the introduction of a controlled amount of the filler. The composites 0 HZS, 4 HZS, 12 HZS, and 19 HZS exhibited closed cell structure with the pores shaped as regular ovals, whereas the sample 25 HZS contained a significant number of open cells with distorted shapes (Fig. 5).

Analysis of the application properties

The application properties of the foams are listed in Table 6. The apparent density (*D*) exhibits a decreasing tendency with higher filler contents in the material but the values are in typical range for RPURFs. The water absorption (*WA*) of the synthesized materials is low, contained in the range of 3.0—3.5 %, which indicates the high share of closed porosity in the sample structure. The dimensional stability (*DS*) of the samples was also exam-

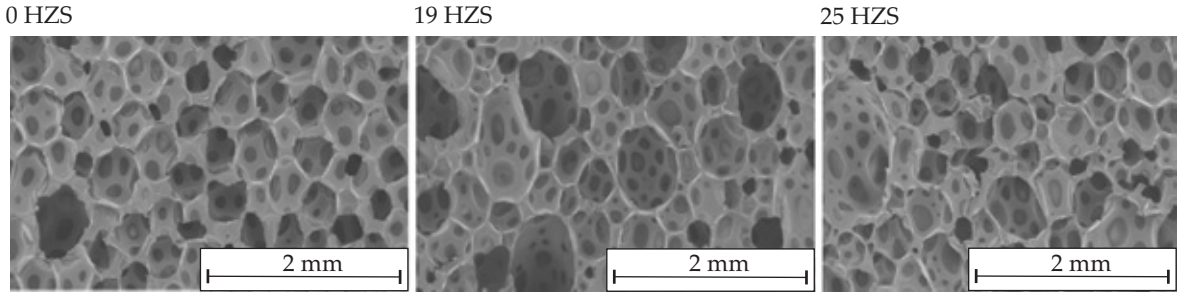

Fig. 5. SEM images of the 0 HZS, 19 HZS, and 25 HZS materials

T a b l e 6. Apparent density, water absorption, and dimensional stability in water and after aging tests

Sample	D, kg/m^3	$WA_{(24\ h,\ 40\ °C)}$, %	$DS_{(24\ h,\ 40\ °C)}$, %	$A_{(48\ h,\ 120\ °C)}$, %
0 HZS	88 ± 2	3.3 ± 0.4	0.6 ± 0.1	0.04 ± 0.01
4 HZS	83 ± 1	3.0 ± 0.5	0.3 ± 0.2	0.09 ± 0.02
12 HZS	79 ± 4	3.5 ± 0.3	0.5 ± 0.1	0.07 ± 0.01
19 HZS	82 ± 2	3.5 ± 0.2	0.4 ± 0.1	0.06 ± 0.01
25 HZS	77 ± 2	3.4 ± 0.3	0.8 ± 0.2	0.08 ± 0.01

ined in a water environment (24 h, 40 °C), as well as after the aging process (48 h, 120 °C – A). The composite containing the greatest amount of the HZS filler exhibited the worst dimensional stability in water. All of the materials were characterized with good resistance to aging conditions. The analyzed parameters are presented in Table 6.

Compressive strength

The compressive strength of the examined materials was investigated in an orientation parallel to the foam growth direction (Fig. 6).

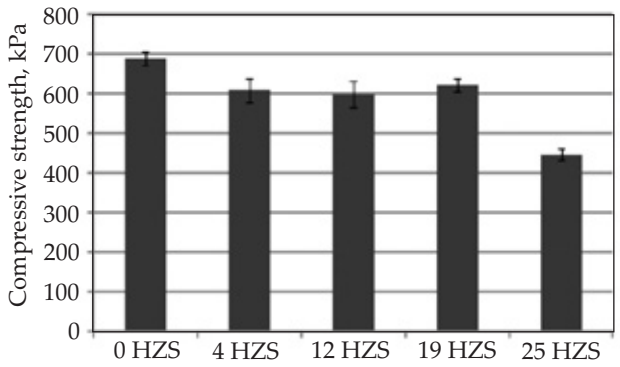

Fig. 6. Compressive strength analysis in orientation parallel to the RPURF growth direction

The 0–19 HZS materials exhibit high values of compressive strength with low deviation, which meets the requirements of the proposed applications. Introduction of greater amounts of the natural filler results in poorer mechanical properties as presented by the 25 HZS composite having 35 % lower compressive strength than the reference material (0 HZS).

Biocompatibility study

The biocompatibility of the examined materials was determined using the *in vitro* toxicity test with application of the human monocyte and human keratinocyte cell lines. The percentage of the cells exhibiting toxic effects in the monocyte line (Km) and in the keratinocyte line (Kk) were determined, as well as the percentage of viable cells in the monocyte line using the neutral red test (Zm).

The overall toxicity of the examined materials was low – below 5 % in the case of human monocyte cell line and below 16 % for human keratinocyte cell line (Table 7). The percentage of viable cells in the neutral red test involving human monocyte cells was higher than 72 % for all of the examined materials. According to the results, the increasing filler content enhances the viability of the cells. The results of the biocompatibility study qualify the examined materials as applicable for use in contact with human skin.

T a b l e 7. Biocompatibility study of examined RPURFs

Sample	Km, %	Kk, %	Zm, %
Control	1.89	10.50	100.00
0 HZS	3.20	5.60	87.52
4 HZS	3.24	15.00	83.17
12 HZS	3.24	7.35	72.32
19 HZS	4.45	5.71	94.31
25 HZS	4.50	6.15	93.94

CONCLUSIONS

The presented research included the synthesis of a series of RPURFs containing 4–25 % by weight of the ground hazelnut shells as a natural filler in the polyol premix. The natural filler grain size distribution indicated that over 90 % of the particles were smaller than 63 μm. The resulting foams were characterized with various macromolecular structures as the introduction of the filler modifies the degree of phase separation and the course of thermal decomposition of the foam materials. Increasing amounts of the natural filler did not significantly alter the apparent density and water absorption of the foams. The dimensional stability after aging was also not changed notably for the desired application of the foams. None of the synthesized foams were found to be toxic.

The 19 HZS material was selected as an optimal product for the cosmetics industry application due to the regular cell structure, high mechanical properties, high biocompatibility, high dimensional stability, and resistance to water environment.

The study has been financed by the National Research and Development Centre within the framework of the project EPURNAT PBS1/B5/18/2012.

REFERENCES

[1] http://www.grandviewresearch.com/industry-analysis/polyurethane-pu-market (data access 08.02.2016)

[2] Zieleniewska M., Leszczyński M.K., Kurańska M. *et al.*: *Industrial Crops and Products* **2015**, *74*, 887. http://dx.doi.org/10.1016/j.indcrop.2015.05.081

[3] Beltrán A.A., Boyacá L.A.: *Latin American Applied Research* **2011**, *41*, 75.

[4] Zhang M., Zhang J., Chen S., Zhou Y.: *Polymer Degradation and Stability* **2014**, *110*, 27. http://dx.doi.org/10.1016/j.polymdegradstab.2014.08.009

[5] Ribeiro da Silva V., Mosiewicki M.A., Yoshida M.I.: *Polymer Testing* **2013**, *32*, 438. http://dx.doi.org/10.1016/j.polymertesting.2013.01.002

[6] Tan S., Abraham T., Ference D., Macosko C.W.: *Polymer* **2011**, *52*, 2840. http://dx.doi.org/10.1016/j.polymer.2011.04.040

[7] Kuranska M., Prociak A.: *Composites Science and Technology* **2012**, *72*, 299. http://dx.doi.org/10.1016/j.compscitech.2011.11.016

[8] Zahedi M., Pirayesh H., Khanjanzdeh H., Tabar M.M.: *Materials and Design* **2013**, *51, 803.* http://dx.doi.org/10.1016/j.matdes.2013.05.007

[9] Dahlke B., Larbig H., Scherzer H.D., Poltrock R.: *Journal of Cellular Plastics* **1998**, *34*, 361.

[10] Gu R., Khazabi M., Sain M.: *BioResources* **2011**, *6* (*4*), 3775.

[11] Sałasińska K., Ryszkowska J.: *Composite Interfaces* **2012**, *19*, 321. http://dx.doi.org/10.1080/15685543.2012.726156

[12] http://www.rosliny.cba.pl/stara/art11.html (data access 08.02.2016)

[13] Medina A.: EU-28 Tree Nuts Annual, USDA Foreign Agricultal Service USA, 2013, Gain report number SP1313.

[14] Ciemieniewska K., Ratusz H.: *Rośliny oleiste* **2012**, *33*, 273.

[15] Sałasińska K.: „Kompozyty polimerowe z napełniaczami pochodzenia roślinnego otrzymywane z materiałów odpadowych", praca doktorska, WUT Base of Knowledge, Warszawa 2014.

[16] Baegazzore D., Alongi J., Frache A.: *Journal of Polymers and the Environment* **2014**, *22*, 88. http://dx.doi.org/10.1007/s10924-013-0616-9

[17] Spear M.J., Eder A., Carus M.: *Wood Composites* **2015**, *10*, 195. http://dx.doi.org/10.1016/B978-1-78242-454-3.00010-X

[18] Balart J.F., Fombuena V., Fenollar O. *et al.*: *Composites Part B: Engineering* **2016**, *86*, 168. http://dx.doi.org/10.1016/j.compositesb.2015.09.063

[19] Matejka V., Fu Z., Kukutschova J. *et al.*: *Materials and Design* **2013**, *51*, 847. http://dx.doi.org/10.1016/j.matdes.2013.04.079

[20] Pretsch T., Jakob I., Muller W.: *Polymer Degradation and Stability* **2009**, *94*, 61. http://dx.doi.org/10.1016/j.polymdegradstab.2008.10.012

[21] Zieleniewska M., Leszczynski M.K., Szczepkowski L. *et al.*: *Polymer Degradation and Stability* **2016**, in press. http://dx.doi.org/10.1016/j.polymdegradstab.2016.02.030

[22] Coleman M.M., Skovanek D.J., Hu J., Painter P.C.: *Macromolecules* **1988**, *21*, 59. http://dx.doi.org/10.1021/ma00179a014

[23] Clift S.M., Grimminger J., Muha K.: "Polyisocyanurate Catalysts for Rigid Polyurethane Foams", SPI Conference 1994, Abstract Number: 112 Session: N.

[24] Ciecierska E., Jurczyk-Kowalska M., Bazarnik P. *et al.*: *Journal of Thermal Analysis and Calorimetry* **2016**, *123*, 283. http://dx.doi.org/10.1007/s10973-015-4940-2

[25] "Szycher's Handbook of Polyurethanes, Second Edition" (Ed. Szycher M.), CRC Press, Boca Raton, USA 2012.

[26] Panthapulakkal S., Sain M.: *Composites Science and Technology* **2010**, *70*, 840.

[27] Fung K.L., Xing X.S., Li R.K.Y. *et al.*: *Composites Science and Technology* **2003**, *63*, 1255.

[28] Manfredi L.B., Rodriguez E.S., Władyka-Przybylak M., Vazquez A.: *Polymer Degradation and Stability* **2006**, *91*, 255. http://dx.doi.org/10.1016/j.polymdegradstab.2005.05.003

[29] Brebu M., Vasile C.: *Cellulose Chemistry and Technology* **2010**, *44*, 353.

Received 27 X 2015.